

# Interference in the resonance fluorescence of two incoherently coupled transitions

Martin Kiffner, Jörg Evers, and Christoph H. Keitel

*Max-Planck-Institut für Kernphysik, Saupfercheckweg 1, 69117 Heidelberg, Germany*

The fluorescence light emitted by a 4-level system in  $J = 1/2$  to  $J = 1/2$  configuration driven by a monochromatic laser field and in an external magnetic field is studied. We show that the spectrum of resonance fluorescence emitted on the  $\pi$  transitions shows a signature of spontaneously generated interference effects. The degree of interference in the fluorescence spectrum can be controlled by means of the external magnetic field, provided that the Landé g-factors of the excited and the ground state doublet are different. For a suitably chosen magnetic field strength, the relative weight of the Rayleigh line can be completely suppressed, even for low intensities of the coherent driving field. The incoherent fluorescence spectrum emitted on the  $\pi$  transitions exhibits a very narrow peak whose width and weight depends on the magnetic field strength. We demonstrate that the spectrum of resonance fluorescence emitted on the  $\sigma$  transitions show an indirect signature of interference. A measurement of the relative peak heights in the spectrum from the  $\sigma$  transitions allows to determine the branching ratio of the spontaneous decay of each excited state into the  $\sigma$  channel.

PACS numbers: 42.50.Ct, 32.50.+d, 42.50.Lc, 42.50.Xa

## I. INTRODUCTION

Since the emergence of quantum mechanics, quantum interference has been regarded as one of the most exciting and intriguing aspects of quantum theory [1]. Although interference effects are present in almost all areas of quantum mechanics, some of them particularly attracted the attention of many scientists. In the following, we will give two examples of physical systems that are well known in the context of interference effects and are both related to the work presented here.

First of all, we would like to mention the so-called V-system that has been intensively discussed by theoretical means. This atomic level scheme is comprised of two near-degenerate excited levels and one ground state, and many authors demonstrated that a rich variety of interference effects should be observable in this system. These effects include the modification and quenching of spontaneous emission [2, 3, 4, 5], and several schemes to control spontaneous emission by means of external fields have been suggested [6, 7, 8, 9]. Furthermore, it has been shown that quantum interference leads to strong modifications of the spectrum of resonance fluorescence, and for suitable parameters the complete suppression of resonance fluorescence is achievable [10, 11, 12, 13]. The emitted fluorescence light also displays highly non-classical features like extremely strong intensity-intensity correlations and squeezing [14, 15].

However, all these schemes rest on the existence of spontaneously generated coherences between the two upper levels that can only arise if the dipole moments between the two upper and the lower level are parallel or at least non-orthogonal. This requirement is very hard to meet in an experiment, since appropriate atomic systems are not known up to now. In order to circumvent this problem, an experiment with a molecular system has been performed [16], but the experimental results could not be reproduced yet [17]. A recent experiment demonstrates the existence of spontaneously generated coher-

ences between spin states in quantum dots [18].

One of the most famous interference effects is certainly Young's double-slit experiment, especially because it allows to explore fundamental concepts of quantum mechanics such as the principle of complementarity in a very simple setup. Celebrated thought experiments like Feynman's light microscope [19] and Einstein's recoiling slits [20] employ the position-momentum uncertainty relation to demonstrate that it is impossible to observe the wave and the particle nature of the interfering quantities (for example, electrons or photons) at the same time. In recent years, a proposal by Scully et. al. [21] gave rise to a lively debate [22, 23, 24, 25, 26, 27, 28] on the interrelation between the principle of complementarity and the position-momentum uncertainty relation.

A beautiful realization of Young's two-slit experiment was performed by Eichmann et. al. [29] and subsequently discussed by several authors [30, 31, 32]. In this experiment, the slits are represented by two  $^{198}\text{Hg}^+$  ions in a trap that are irradiated by a coherent laser field, and the interference pattern formed by the scattered light was observed. The level scheme of each of the two atoms can be modeled by a  $J = 1/2$  to  $J = 1/2$  transition that is also in the focus of the work presented here; a schematic representation of this four-level system is shown in Fig. 1 [33, 34, 35]. The transitions  $|1\rangle \leftrightarrow |4\rangle$  and  $|2\rangle \leftrightarrow |3\rangle$  couple to  $\sigma^+$  and  $\sigma^-$  polarized light, respectively, and will be referred to as the  $\sigma$  transitions. By contrast, the  $\pi$  transitions  $|1\rangle \leftrightarrow |3\rangle$  and  $|2\rangle \leftrightarrow |4\rangle$  couple to light linearly polarized along  $e_z$ , and their dipole moments are anti-parallel. The four-level system of Fig. 1 is thus a realistic level scheme with non-orthogonal dipole moments which can be found in real atoms. However, it cannot be expected that this four-level system displays the same interference effects that were predicted for the V-system with parallel dipole moments since there is a striking difference between them. In the case of the V-system, both transitions from the upper levels end up in the same ground state, while the

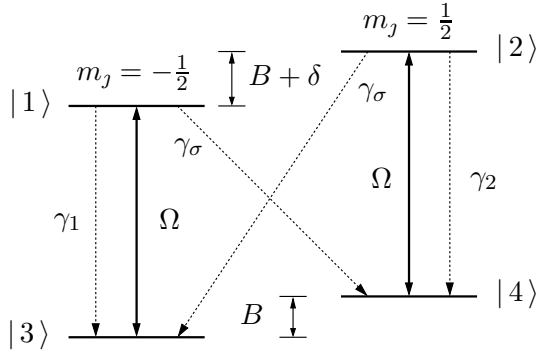


FIG. 1: Schematic representation of the four-level atom of interest. The two upper and lower levels are Zeeman sub-levels with  $m_J = \pm \frac{1}{2}$ . Each upper state can decay by a dipole allowed transition to both ground states. The Zeeman splitting of the magnetic sub-levels is not to scale.

two  $\pi$  transitions of our four-level system start and end up in different states that are orthogonal to each other. Thus the question arises whether interference effects can also be observed in single  $J = 1/2$  to  $J = 1/2$  systems.

Recently we investigated the fluorescence light emitted on the  $\pi$  transitions in the case of the *degenerate* system ( $B = \delta = 0$  in Fig. 1) and for a monochromatic driving field polarized along  $\mathbf{e}_z$ . It has been shown [36] that the spectrum of resonance fluorescence indeed exhibits a signature of vacuum-mediated interference effects, whereas the total intensity is not affected by interference. It has been demonstrated that this result is a consequence of the principle of complementarity, applied to time and energy.

Here we generalize our analysis to the non-degenerate system depicted in Fig. 1 and include the fluorescence light emitted on the  $\sigma$  transitions in our discussion. Since it is possible to discriminate between the fluorescence light that stems from the  $\pi$ - and the  $\sigma$  transitions simply by means of a polarization-dependent detection scheme (Sec. II), these two contributions will be discussed independently in Secs. III and IV, respectively.

We find that for the spectrum from the  $\pi$  transitions, the degree of interference in the coherent and incoherent part of the spectrum strongly depends on the frequency difference  $\delta$  between the two  $\pi$  transitions. The spectral properties of the fluorescence light can thus be controlled by means of an external magnetic field that determines the value of  $\delta$ . For example, the relative weight of the Rayleigh line can be completely suppressed for a suitable value of  $\delta$ , even for low intensities of the coherent driving field (Sec. III A). The dependence of the incoherent spectrum of resonance fluorescence on the parameter  $\delta$  is discussed in Sec. III B. Section III C demonstrates how the interference terms alter the fluorescence spectrum emitted on the  $\pi$  transitions for different regimes of the driving field strength. The experimental observation of the spectra including the interference terms could pro-

vide evidence for vacuum-mediated interference effects in an atomic system.

The fluorescence spectrum emitted on the  $\sigma$  transitions of the degenerate system is discussed in Sec. IV. It only consists of an incoherent part and shows an indirect signature of interference since the relative peak heights depend on the interference terms. The measurement of the relative peak heights would also allow to determine the branching ratio of the spontaneous decay of each excited state into the  $\sigma$  channel.

Section V provides a detailed discussion of our results. In our previous work [36], we interpreted the interference effect in the spectrum of resonance fluorescence in terms of interferences between transition amplitudes that correspond to different time orders of photon emissions. Here we support this explanation by a formal argument, and the continuous transition from perfect frequency resolution to perfect temporal resolution is studied in more detail. For a weak driving field and certain values of the parameter  $\delta$ , the incoherent spectra of the  $\pi$  and  $\sigma$  transitions contain a very narrow peak whose width is smaller than the natural linewidth. We explain these narrow structures in terms of electron shelving. Finally, a brief summary of our results is given in Sec. VI.

## II. EQUATION OF MOTION AND DETECTION SCHEME

We now return to the level scheme in Fig. 1. Note that we allow the Zeeman splitting of the excited and the ground state magnetic sub-levels to be different, since the Landé g-factors will not necessarily be the same for these two multiplets. For example, in the case of the  $6s^2 S_{1/2} - 6p^2 P_{1/2}$  transition in  $^{198}\text{Hg}^+$  the g-factor for the excited states is given by  $2/3$ , and for the ground states it takes on its maximum value of  $2$ . The matrix elements of the electric-dipole moment operator  $\hat{\mathbf{d}}$  can be found from the Wigner-Eckart theorem [37] and are given by

$$\begin{aligned} \mathbf{d}_1 &= \langle 1 | \hat{\mathbf{d}} | 3 \rangle = -\frac{1}{\sqrt{3}} \mathcal{D} \mathbf{e}_z, & \mathbf{d}_2 &= \langle 2 | \hat{\mathbf{d}} | 4 \rangle = -\mathbf{d}_1 \\ \mathbf{d}_3 &= \langle 2 | \hat{\mathbf{d}} | 3 \rangle = \sqrt{\frac{2}{3}} \mathcal{D} \mathbf{\epsilon}^{(-)}, & \mathbf{d}_4 &= \langle 1 | \hat{\mathbf{d}} | 4 \rangle = \mathbf{d}_3^*. \end{aligned} \quad (1)$$

In this equation, the circular polarization vector is defined as  $\mathbf{\epsilon}^{(-)} = (\mathbf{e}_x - i\mathbf{e}_y)/\sqrt{2}$  and  $\mathcal{D}$  denotes the reduced dipole matrix element. We assign to each of the four dipole-allowed transitions a resonance frequency  $\omega_i$  ( $i \in \{1, 2, 3, 4\}$ ). If the splitting between the magnetic sub-levels vanishes (i.e.  $B = \delta = 0$ ), these four frequencies are equal.

We are interested in the time evolution of our four level system driven by a monochromatic field of frequency  $\omega_L$  that is linearly polarized along the  $z$  axis,

$$\mathbf{E}(t) = E_0 e^{-i\omega_L t} \mathbf{e}_z + \text{c.c.}, \quad (2)$$

and c.c. stands for the complex conjugate. With this choice of polarization, the electric field couples only to the two anti-parallel dipole moments  $\mathbf{d}_1$  and  $\mathbf{d}_2$ . In the rotating wave approximation, the interaction Hamiltonian takes the form

$$V = (A_{13} - A_{24}) \hbar \Omega e^{-i\omega_L t} + \text{h.c.}, \quad (3)$$

where the atomic transition operators are defined as  $A_{ij} = |i\rangle\langle j|$ , and the Rabi frequency is given by  $\Omega = E_0 \mathcal{D}/(\sqrt{3} \hbar)$ . The atomic Hamiltonian can be written as

$$H_0 = \hbar \omega_1 A_{11} + \hbar(\omega_2 + B) A_{22} + \hbar B A_{44}, \quad (4)$$

where  $\omega_1$  stands for the resonance frequency of the  $1 \leftrightarrow 3$  transition and  $\omega_2 = \omega_1 + \delta$  is the resonance frequency on the  $2 \leftrightarrow 4$  transition. In a rotating frame defined by the unitary transformation

$$W = \exp [ (A_{11} + A_{22}) i \omega_L t ], \quad (5)$$

the master equation for the density operator  $\tilde{\varrho} = W \varrho W^\dagger$  reads

$$\dot{\tilde{\varrho}} = -\frac{i}{\hbar} [H, \tilde{\varrho}] + \mathcal{L}_\gamma \tilde{\varrho}. \quad (6)$$

In this equation, the Hamiltonian is given by

$$H = -\hbar [\Delta A_{11} + (\Delta - \delta) A_{22} - B (A_{22} + A_{44})] + [(A_{13} - A_{24}) \hbar \Omega + \text{h.c.}], \quad (7)$$

$\Delta = \omega_L - \omega_1$  is the detuning of the driving field from resonance with the  $1 \leftrightarrow 3$  transition,  $\Delta - \delta$  is the detuning on the  $2 \leftrightarrow 4$  transition and the damping term  $\mathcal{L}_\gamma \tilde{\varrho}$  takes the form

$$\begin{aligned} \mathcal{L}_\gamma \tilde{\varrho} = & -\frac{1}{2} \sum_{i,j=1}^2 \gamma_{ij} \{ [S_i^+, S_j^- \tilde{\varrho}] + [\tilde{\varrho} S_i^+, S_j^-] \} \\ & - \frac{\gamma_\sigma}{2} \sum_{i=3}^4 \{ [S_i^+, S_i^- \tilde{\varrho}] + [\tilde{\varrho} S_i^+, S_i^-] \}. \end{aligned} \quad (8)$$

The transition operators  $S_i^\pm$  are defined as

$$S_1^+ = A_{13}, \quad S_2^+ = A_{24}, \quad S_3^+ = A_{23}, \quad S_4^+ = A_{14}, \quad (9)$$

and  $S_i^- = (S_i^+)^{\dagger}$ . The decay constant on each of the  $\sigma$  transitions is denoted by  $\gamma_\sigma$ , the parameters  $\gamma_{ij}$  are determined by

$$\gamma_{ij} = \frac{\mathbf{d}_i \cdot \mathbf{d}_j^*}{|\mathbf{d}_i| |\mathbf{d}_j|} \sqrt{\gamma_i \gamma_j} \quad i, j \in \{1, 2\}, \quad (10)$$

and  $\gamma_1$  and  $\gamma_2$  are the decay constants of the  $\pi$  transitions (see Fig. 1). For  $i = j$ , the parameters  $\gamma_{ij}$  are equal to the decay rates of the  $\pi$  transitions,  $\gamma_{11} = \gamma_1$  and  $\gamma_{22} = \gamma_2$ . Although  $\gamma_1$  and  $\gamma_2$  are equal in our

setup, we will continue to label them differently to facilitate the physical interpretation later on. Since  $\hat{\mathbf{d}}_1$  and  $\hat{\mathbf{d}}_2$  are anti-parallel, the cross-damping terms are given by  $\gamma_{12} = \gamma_{21} = -\sqrt{\gamma_1 \gamma_2}$ . These terms allow for the possibility of coherence transfer from the excited to the ground state doublet.

The decay rates  $\gamma_1, \gamma_2, \gamma_\sigma$  can be related to the total decay rate  $\gamma = \gamma_1 + \gamma_\sigma = \gamma_2 + \gamma_\sigma$  of each of the two excited states through the branching probabilities  $b_\pi$  and  $b_\sigma$ ,

$$\gamma_1 = \gamma_2 = b_\pi \gamma \quad \text{and} \quad \gamma_\sigma = b_\sigma \gamma. \quad (11)$$

According to the Clebsch-Gordan coefficients, we have  $b_\pi = 1/3$  and  $b_\sigma = 2/3$ . Although we will keep the symbols  $b_\pi$  and  $b_\sigma$  in formulas, we will always assume these values whenever a concrete evaluation is performed, e.g. in figures.

Next we employ the normalization condition  $\text{Tr}(\tilde{\varrho}) = 1$  to eliminate the matrix element  $\tilde{\varrho}_{44}$  from the master equation (6) that can be cast into the form

$$\partial_t \mathbf{R}(t) = \mathcal{M} \mathbf{R}(t) + \mathbf{I}. \quad (12)$$

Here  $\mathcal{M}$  represents a generalized  $15 \times 15$  Bloch matrix, the vector  $\mathbf{I}$  is an inhomogeneity with components

$$\mathbf{I} = (0, 0, 0, 0, 0, 0, 0, i \Omega, 0, 0, 0, 0, 0, -i \Omega^*, 0)^t \quad (13)$$

and the vector  $\mathbf{R}$  contains the matrix elements  $\tilde{\varrho}_{ij} = \langle i | \tilde{\varrho} | j \rangle$  of the density operator,

$$\begin{aligned} \mathbf{R} = & (\tilde{\varrho}_{11}, \tilde{\varrho}_{12}, \tilde{\varrho}_{13}, \tilde{\varrho}_{14}, \tilde{\varrho}_{21}, \tilde{\varrho}_{22}, \tilde{\varrho}_{23}, \tilde{\varrho}_{24}, \\ & \tilde{\varrho}_{31}, \tilde{\varrho}_{32}, \tilde{\varrho}_{33}, \tilde{\varrho}_{34}, \tilde{\varrho}_{41}, \tilde{\varrho}_{42}, \tilde{\varrho}_{43})^t. \end{aligned} \quad (14)$$

The stationary solution of Eq. (12) is formally given by

$$\mathbf{R}_{\text{st}} = -\mathcal{M}^{-1} \mathbf{I}, \quad (15)$$

and an evaluation of the latter equation yields

$$\begin{aligned} \tilde{\varrho}_{11} &= \frac{1}{2} \frac{|\Omega|^2}{\gamma^2/4 + \delta^2/4 + (\Delta - \delta/2)^2 + 2|\Omega|^2} \\ \tilde{\varrho}_{33} &= \frac{1}{2} \frac{\gamma^2/4 + \Delta^2 + |\Omega|^2}{\gamma^2/4 + \delta^2/4 + (\Delta - \delta/2)^2 + 2|\Omega|^2} \\ \tilde{\varrho}_{44} &= \frac{1}{2} \frac{\gamma^2/4 + (\Delta - \delta)^2 + |\Omega|^2}{\gamma^2/4 + \delta^2/4 + (\Delta - \delta/2)^2 + 2|\Omega|^2} \\ \tilde{\varrho}_{13} &= \frac{1}{2} \frac{(\Delta - i\gamma/2) \Omega}{\gamma^2/4 + \delta^2/4 + (\Delta - \delta/2)^2 + 2|\Omega|^2} \\ \tilde{\varrho}_{24} &= \frac{1}{2} \frac{(\delta - \Delta + i\gamma/2) \Omega}{\gamma^2/4 + \delta^2/4 + (\Delta - \delta/2)^2 + 2|\Omega|^2}. \end{aligned} \quad (16)$$

The remaining non-zero components of  $\mathbf{R}_{\text{st}}$  are determined by

$$\tilde{\varrho}_{11} = \tilde{\varrho}_{22}, \quad \tilde{\varrho}_{31} = \tilde{\varrho}_{13}^* \quad \text{and} \quad \tilde{\varrho}_{42} = \tilde{\varrho}_{24}^*. \quad (17)$$

In the case of the degenerate system, the population of the two ground levels will be equal and we have  $\tilde{\varrho}_{13} = -\tilde{\varrho}_{24}$ . Note that the minus sign arises since the dipole moments  $\mathbf{d}_1$  and  $\mathbf{d}_2$  are anti-parallel, and the coherences  $\tilde{\varrho}_{14}$  and  $\tilde{\varrho}_{23}$  are equal to zero because the driving field does not couple to the  $\sigma$  transitions.

In this paper we focus on the total intensity and the spectral distribution of the fluorescence light emitted by the atom in steady state. The total intensity

$$I_{\text{st}} = \langle \hat{\mathbf{E}}^{(-)}(\mathbf{r}, t) \cdot \hat{\mathbf{E}}^{(+)}(\mathbf{r}, t) \rangle_{\text{st}} \quad (18)$$

is given by the normally ordered first-order correlation function of the electric field, and the spectrum of resonance fluorescence is determined by the Fourier transform of the two-time correlation function of the electric field [38],

$$S(\omega) = \frac{1}{2\pi} \int_{-\infty}^{\infty} e^{-i\omega\tau} \langle \hat{\mathbf{E}}^{(-)}(\mathbf{r}, t + \tau) \cdot \hat{\mathbf{E}}^{(+)}(\mathbf{r}, t) \rangle_{\text{st}} d\tau. \quad (19)$$

In these equations,  $\hat{\mathbf{E}}^{(-)} \left( \hat{\mathbf{E}}^{(+)} \right)$  denotes the negative (positive) frequency part of the electric field operator. At a point  $\mathbf{r} = r\hat{\mathbf{r}}$  in the far-field zone, the negative frequency part of the electric field operator is found to be [2]

$$\begin{aligned} \hat{\mathbf{E}}^{(-)}(\mathbf{r}, t) &= \hat{\mathbf{E}}_{\text{free}}^{(-)}(\mathbf{r}, t) \\ &\quad - \frac{\eta}{r} \sum_{i=1}^4 \omega_i^2 \hat{\mathbf{r}} \times (\hat{\mathbf{r}} \times \mathbf{d}_i) \tilde{S}_i^+(\hat{t}) e^{i\omega_L \hat{t}}, \end{aligned} \quad (20)$$

where  $\hat{t} = t - \frac{r}{c}$  is the retarded time,  $\eta = 1/(4\pi\varepsilon_0 c^2)$  and  $\tilde{S}_i^\pm = \exp(\mp i\omega_L t) S_i^\pm$ . The first term stands for the negative frequency part of the free field. It does not contribute to the normally ordered correlation functions in Eqs. (18) and (19) as long as the point of observation lies outside the driving field [39]. The second term describes the retarded dipole field generated by the atom situated at the point of origin.

Throughout this paper we assume that the point of observation lies in the  $y$ -direction, where the  $z$ - and  $x$ -axes are defined by the polarization and the direction of propagation of the laser beam, respectively. An evaluation of the cross products in Eq. (20) shows then that the light emitted on the  $\pi$  transitions is linearly polarized along  $\mathbf{e}_z$ , whereas the light emitted on the  $\sigma$  transitions is linearly polarized along  $\mathbf{e}_x$ . The advantage of this detection scheme is that one can easily discriminate between the light emitted on the  $\pi$  and  $\sigma$  transitions by means of a polarization filter. For this reason we will discuss the fluorescence light of the  $\pi$ -and  $\sigma$  transitions separately.

### III. SPECTRUM OF RESONANCE FLUORESCENCE – $\pi$ TRANSITIONS

We begin with a brief discussion of the steady-state intensity recorded by a broadband detector that observes the light emitted on the  $\pi$  transitions. According to Eqs. (18) and (20), we have

$$I_{\text{st}}^\pi = \phi_\pi \sum_{i,j=1}^2 \gamma_{ij} \langle \tilde{S}_i^+ \tilde{S}_j^- \rangle_{\text{st}}, \quad (21)$$

where it was assumed that  $\omega_1 \approx \omega_2$  to obtain a common prefactor  $\phi_\pi$  that we set equal to one in the following. The terms  $\gamma_{ij}$  are defined in Eq. (10), and  $\gamma_{12} = \gamma_{21} = -\sqrt{\gamma_1 \gamma_2}$  describe the cross-damping between the  $\pi$  transitions that arises as a consequence of quantum interference. However, these interference terms do not contribute to the total intensity, regardless of what the steady state solution might be, because the ground states are orthogonal,

$$\langle \tilde{S}_1^+ \tilde{S}_2^- \rangle_{\text{st}} = \langle |1\rangle \langle 3| |4\rangle \langle 2| \rangle_{\text{st}} = 0. \quad (22)$$

Consequently, the intensity emitted on the  $\pi$  transitions is not altered by interference terms and simply proportional to the population of the excited states,

$$I_{\text{st}}^\pi = b_\pi \gamma (\tilde{\varrho}_{11} + \tilde{\varrho}_{22}). \quad (23)$$

We now turn to the the spectrum of resonance fluorescence emitted on the  $\pi$  transitions. With the help of Eqs. (19) and (20) we arrive at

$$S^\pi(\tilde{\omega}) = \frac{1}{\pi} \sum_{i,j=1}^2 \gamma_{ij} \text{Re} \int_0^\infty e^{-i\tilde{\omega}\tau} \langle \tilde{S}_i^+(\hat{t} + \tau) \tilde{S}_j^-(\hat{t}) \rangle_{\text{st}} d\tau, \quad (24)$$

where  $\tilde{\omega} = \omega - \omega_L$  is the difference between the observed frequency and the laser frequency. In contrast to Eq. (22), the terms proportional to  $\gamma_{12}$  are now determined by the *two-time averages*  $\langle \tilde{S}_1^+(\hat{t} + \tau) \tilde{S}_2^-(\hat{t}) \rangle_{\text{st}}$  rather than by the one-time averages. Indeed, we find that the correlation function

$$G_{12}(\tau) = -\sqrt{\gamma_1 \gamma_2} \langle \tilde{S}_1^+(\hat{t} + \tau) \tilde{S}_2^-(\hat{t}) \rangle_{\text{st}} \quad (25)$$

is different from zero for  $\tau > 0$ ; a plot of  $G_{12}$  is shown in Fig. 2. But this implies that there is quantum interference in the spectrum of the light emitted on the  $\pi$  transitions, although there is no interference in the total intensity. To illustrate this result we decompose the transition operators in Eq. (25) in mean values and fluctuations according to

$$\tilde{S}_i^\pm = \langle \tilde{S}_i^\pm \rangle_{\text{st}} \hat{1} + \delta \tilde{S}_i^\pm. \quad (26)$$

The correlation function  $G_{12}(\tau)$  becomes then

$$\begin{aligned} G_{12}(\tau) &= -\sqrt{\gamma_1 \gamma_2} \left[ \langle \delta \tilde{S}_1^+(\hat{t} + \tau) \delta \tilde{S}_2^-(\hat{t}) \rangle_{\text{st}} \right. \\ &\quad \left. + \langle \tilde{S}_1^+ \rangle_{\text{st}} \langle \tilde{S}_2^- \rangle_{\text{st}} \right]. \end{aligned} \quad (27)$$

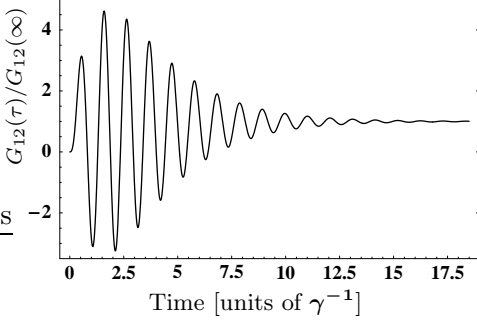


FIG. 2: Plot of the correlation function  $G_{12}$  in relation to its long-time limit  $G_{12}(\infty) = -\sqrt{\gamma_1 \gamma_2} \langle \tilde{S}_1^+ \rangle_{\text{st}} \langle \tilde{S}_2^- \rangle_{\text{st}}$  for the degenerate system. The parameters are  $\Omega = 3 \times 10^7 \text{ s}^{-1}$ ,  $\Delta = 5 \times 10^6 \text{ s}^{-1}$  and  $\gamma = 10^7 \text{ s}^{-1}$ .  $G_{12}$  has to vanish at  $\tau = 0$  since the ground states are orthogonal.

The two-time average of the fluctuations can be calculated from the generalized Bloch equations and the quantum regression theorem (see Appendix). It decays exponentially with a time constant on the order of  $\gamma^{-1}$  and does not contribute to  $G_{12}$  in the long-time limit  $\tau \rightarrow \infty$ . The mean values  $\langle \tilde{S}_1^+ \rangle_{\text{st}} = \tilde{\varrho}_{31}$  and  $\langle \tilde{S}_2^+ \rangle_{\text{st}} = \tilde{\varrho}_{42}$  are given by matrix elements of the steady-state density-operator in Eq. (16) and are both different from zero. This is obvious from a physical point of view since the laser field creates a coherence on both transitions  $1 \leftrightarrow 3$  and  $2 \leftrightarrow 4$ . Consequently, the long-time limit of  $G_{12}$  reads  $G_{12}(\infty) = -\sqrt{\gamma_1 \gamma_2} \langle \tilde{S}_1^+ \rangle_{\text{st}} \langle \tilde{S}_2^- \rangle_{\text{st}}$ . It follows that the interference terms will affect the coherent and incoherent spectrum of resonance fluorescence.

Before we give expressions for the spectral distribution of the emitted light, we calculate the respective contributions of coherent and incoherent scattering to the intensity  $I_{\text{st}}^\pi$ . To this end we apply the decomposition of the transition operators Eq. (26) to Eq. (21). This allows us to write  $I_{\text{st}}^\pi$  as the sum of four terms,

$$I_{\text{st}}^\pi = I_{\text{coh}}^0 + I_{\text{coh}}^{\text{int}} + I_{\text{inc}}^0 + I_{\text{inc}}^{\text{int}}. \quad (28)$$

The first two terms account for the contribution of coherent scattering (subscript ‘‘coh’’) and are given by

$$I_{\text{coh}}^0 = \gamma_1 |\langle \tilde{S}_1^+ \rangle_{\text{st}}|^2 + \gamma_2 |\langle \tilde{S}_2^+ \rangle_{\text{st}}|^2 \quad (29)$$

$$I_{\text{coh}}^{\text{int}} = -2 \sqrt{\gamma_1 \gamma_2} \text{Re} \langle \tilde{S}_1^+ \rangle_{\text{st}} \langle \tilde{S}_2^- \rangle_{\text{st}}. \quad (30)$$

In this equation,  $I_{\text{coh}}^0$  stands for the contribution of terms proportional to  $\gamma_{11}$  and  $\gamma_{22}$ , and  $I_{\text{coh}}^{\text{int}}$  is the weight of the interference terms that can be positive or negative. By contrast, the sum of  $I_{\text{coh}}^0$  and  $I_{\text{coh}}^{\text{int}}$  is the weight of the Rayleigh line that is always positive. The last two terms in Eq. (28) denote the contribution of incoherent scattering (subscript ‘‘inc’’),

$$I_{\text{inc}}^0 = \gamma_1 \langle \delta \tilde{S}_1^+ \delta \tilde{S}_1^- \rangle_{\text{st}} + \gamma_2 \langle \delta \tilde{S}_2^+ \delta \tilde{S}_2^- \rangle_{\text{st}} \quad (31)$$

$$I_{\text{inc}}^{\text{int}} = -2 \sqrt{\gamma_1 \gamma_2} \text{Re} \langle \delta \tilde{S}_1^+ \delta \tilde{S}_2^- \rangle_{\text{st}}. \quad (32)$$

Since the ground states are orthogonal, Eq. (26) allows to establish the relation

$$\langle \delta \tilde{S}_1^+ \delta \tilde{S}_2^- \rangle_{\text{st}} = -\langle \tilde{S}_1^+ \rangle_{\text{st}} \langle \tilde{S}_2^- \rangle_{\text{st}}. \quad (33)$$

If this expression is applied to Eq. (32), it follows from Eq. (30) that the interference terms  $I_{\text{coh}}^{\text{int}}$  and  $I_{\text{inc}}^{\text{int}}$  are of opposite sign, i.e.

$$I_{\text{coh}}^{\text{int}} = -I_{\text{inc}}^{\text{int}}. \quad (34)$$

This relation clarifies that the interference terms alter the weights of the coherent and the incoherent part of the spectrum, whereas the total intensity remains unchanged. Note that this is in contrast to the V-system with non-orthogonal transition dipole moments mentioned in the introduction, where both the fluorescence spectrum and the total intensity show a signature of interference [1, 3, 12, 13].

We now turn to the spectral distribution of the fluorescence light and employ Eq. (26) to write the spectrum of resonance fluorescence in Eq. (24) as the sum of the coherent and the incoherent spectrum,  $S^\pi(\tilde{\omega}) = S_{\text{coh}}^\pi(\tilde{\omega}) + S_{\text{inc}}^\pi(\tilde{\omega})$ , where

$$S_{\text{coh}}^\pi(\tilde{\omega}) = (I_{\text{coh}}^0 + I_{\text{coh}}^{\text{int}}) \delta(\tilde{\omega}) \quad (35)$$

$$S_{\text{inc}}^\pi(\tilde{\omega}) = \frac{1}{\pi} \sum_{i,j=1}^2 \gamma_{ij} \text{Re} \int_0^\infty e^{-i\tilde{\omega}\tau} \langle \delta \tilde{S}_i^+ (\hat{t} + \tau) \delta \tilde{S}_j^- (\hat{t}) \rangle_{\text{st}} d\tau. \quad (36)$$

These two contributions will be discussed in the following Sections.

### A. Coherent spectrum of resonance fluorescence

The coherent part of the fluorescence spectrum consists of the Rayleigh peak centered at  $\omega = \omega_L$ . In order to get a better understanding of how the weight of this line is affected by interference, we write it as

$$I_{\text{coh}}^0 + I_{\text{coh}}^{\text{int}} = |\sqrt{\gamma_1} \langle \tilde{S}_1^+ \rangle_{\text{st}} - \sqrt{\gamma_2} \langle \tilde{S}_2^+ \rangle_{\text{st}}|^2. \quad (37)$$

In this equation,  $\langle \tilde{S}_1^+ \rangle_{\text{st}}$  is proportional to the scattering amplitude on the  $1 \leftrightarrow 3$  transition and  $-\langle \tilde{S}_2^+ \rangle_{\text{st}}$  corresponds to the scattering amplitude on the  $2 \leftrightarrow 4$  transition. Note that the minus sign arises since the dipoles  $\mathbf{d}_1$  and  $\mathbf{d}_2$  are anti-parallel. Depending on the relative phase and the absolute values of the coherences  $\langle \tilde{S}_1^+ \rangle_{\text{st}}$  and  $\langle \tilde{S}_2^+ \rangle_{\text{st}}$ , there will be constructive or destructive interference in the coherent part of the spectrum. We will now demonstrate that the degree of interference in the coherent spectrum can be controlled by means of the difference  $\delta$  between the resonance frequencies of the  $\pi$  transitions. Therefore, we write Eq. (37) as

$$I_{\text{coh}}^0 + I_{\text{coh}}^{\text{int}} = I_{\text{coh}}^0 [1 + C], \quad (38)$$

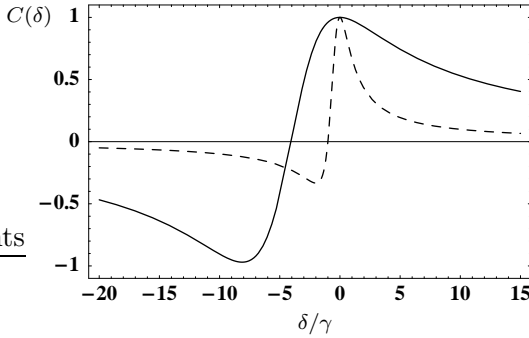


FIG. 3: Plot of the relative weight of the interference terms  $C(\delta)$  for different values of the detuning  $\Delta$  of the laser field from the  $1 \leftrightarrow 3$  transition. The parameters are given by  $\gamma = 10^7 \text{ s}^{-1}$ ,  $\Delta = -4 \times 10^7 \text{ s}^{-1}$  (solid line) and  $\Delta = -5 \times 10^6 \text{ s}^{-1}$  (dashed line).

where  $C = I_{\text{coh}}^{\text{int}}/I_{\text{coh}}^0$  is the relative weight of the interference terms. An explicit expression for  $C$  can be found with the help of the definitions in Eq. (30) and the steady-state solution for  $\tilde{\varrho}$  in Eq. (16),

$$C = \frac{\gamma^2/4 + \Delta(\Delta - \delta)}{\gamma^2/4 + \delta^2/4 + (\Delta - \delta/2)^2}. \quad (39)$$

The absolute value of this quantity can be regarded as the degree of interference in the coherent spectrum. Figure 3 shows a plot of  $C$  as a function of  $\delta$  for two different (negative) detunings  $\Delta$ . It is evident that  $C$  is equal to one in the case of the degenerate system. Therefore, we have perfect constructive interference for  $\delta = 0$ . In this case, the detunings on both  $\pi$  transitions are equal and hence we have  $\langle \tilde{S}_1^+ \rangle_{\text{st}} = -\langle \tilde{S}_2^+ \rangle_{\text{st}}$ , the two transitions are now perfectly equivalent. In addition, the weight of the Rayleigh line is then, apart from the branching probability  $b_\pi$ , identical to the corresponding expression for a two-level atom [40].

As  $|\delta|$  increases,  $C(\delta)$  decreases monotonously and becomes zero at  $\delta_0 = \Delta[1 + \gamma^2/(4\Delta^2)]$ . Note that  $\delta_0$  can be either positive or negative, depending on the sign of  $\Delta$ . In the case of  $\Delta^2 \gg \gamma^2$ , we have  $\delta_0 \approx \Delta$ . This implies that the interference term vanishes if the laser field is resonant with the  $2 \leftrightarrow 4$  transition. The minimum of the curve is reached at  $\delta_{\min} = 2\Delta(1 + \gamma^2/(4\Delta^2))$  and given by  $C(\delta_{\min}) = -1/(1 + \gamma^2/(2\Delta^2))$ . Consequently,  $C(\delta_{\min})$  tends to  $-1$  provided that  $\Delta^2 \gg \gamma^2$ . The weight of the Rayleigh peak becomes then zero as a consequence of destructive interference, and the emitted radiation is solely incoherent. Note that this situation occurs if the detunings on the  $1 \leftrightarrow 3$  and  $2 \leftrightarrow 4$  transitions are approximately equal and of opposite sign. In this case, the coherences  $\langle \tilde{S}_1^+ \rangle_{\text{st}}$  and  $\langle \tilde{S}_2^+ \rangle_{\text{st}}$  cancel each other in Eq. (37). Finally,  $C$  tends to zero as  $|\delta|$  becomes much larger than  $|\Delta|$  and  $\gamma$ . This is due to the fact that the interference term in Eq. (30) consists of the product of  $\langle \tilde{S}_1^+ \rangle_{\text{st}}$  and  $\langle \tilde{S}_2^+ \rangle_{\text{st}}$ . If the detuning on one of the

two  $\pi$  transitions becomes very large,  $I_{\text{coh}}^{\text{int}}$  tends to zero, whereas  $I_{\text{coh}}^0$  remains different from zero.

## B. Incoherent spectrum of resonance fluorescence

It is possible to evaluate the expression for  $S_{\text{inc}}^\pi$  in Eq. (36) analytically, an outline of the calculation can be found in the Appendix. However, the general result is too bulky to present it here. We just mention that the spectrum does only depend on the difference  $\delta$  between the Zeeman splittings of the ground and excited states, but not on the parameter  $B$  (see Fig. 1). In the case of the degenerate system, we find

$$S_{\text{inc}}^\pi(\tilde{\omega}) = b_\pi \frac{\gamma}{\pi} \frac{\gamma^2 + 2|\Omega|^2 + \tilde{\omega}^2}{\gamma^2/4 + \Delta^2 + 2|\Omega|^2} \frac{2\gamma|\Omega|^4}{|P(-i\tilde{\omega})|^2}, \quad (40)$$

where  $P(z)$  is a cubic polynomial as a function of  $z$  that is defined as

$$P(z) = \frac{1}{4}(z + \gamma)[(2z + \gamma)^2 + 4\Delta^2] + 2(2z + \gamma)|\Omega|^2. \quad (41)$$

Apart from the branching probability  $b_\pi$ , this result is *exactly* the same as the incoherent spectrum of resonance fluorescence of a two-level atom [40].

As soon as  $\delta$  becomes different from zero, the incoherent spectrum differs considerably from the two-level spectrum. This is demonstrated in Fig. 4 a) which displays  $S_{\text{inc}}^\pi$  for  $\delta = 0$  (dashed line) and  $\delta = -4 \times 10^6 \text{ s}^{-1}$  (solid line). For  $\delta \neq 0$ , an additional central peak occurs whose width is much smaller than the decay rate  $\gamma$ .

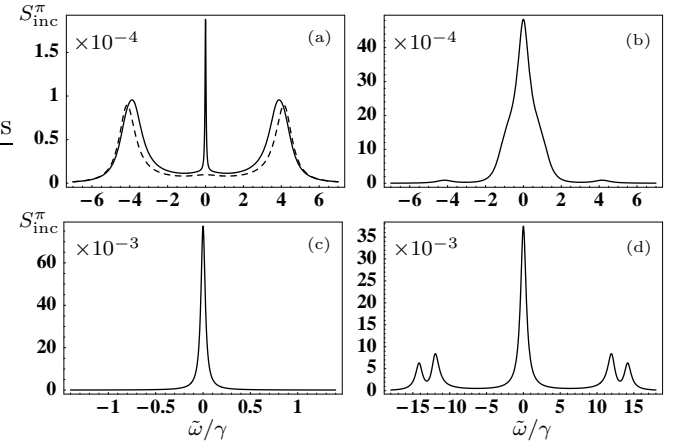


FIG. 4: Incoherent spectrum of resonance fluorescence according to Eq. (36). Plot (a) shows  $S_{\text{inc}}^\pi$  for the degenerate system (dashed line) and for  $\delta = -4 \times 10^6 \text{ s}^{-1}$  (solid line), the other parameters are  $\gamma = 10^7 \text{ s}^{-1}$ ,  $\Delta = -4 \times 10^7 \text{ s}^{-1}$  and  $\Omega = 6 \times 10^6 \text{ s}^{-1}$ . In (b) and (c) the values of  $\delta$  are given by  $\delta = \delta_0$  and  $\delta = \delta_{\min}$ , respectively, the other parameters are the same than in (a). Plot (d) shows the incoherent spectrum for the set of parameters  $\Delta = -5 \times 10^6 \text{ s}^{-1}$ ,  $\Omega = 6 \times 10^7 \text{ s}^{-1}$ ,  $\gamma = 10^7 \text{ s}^{-1}$  and  $\delta = -8 \times 10^7 \text{ s}^{-1}$ .

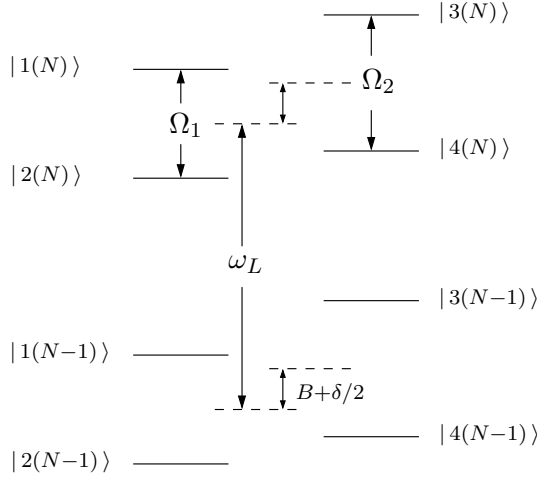


FIG. 5: Dressed state analog of the bare state system in Fig. 1. The frequency of the laser field is labeled by  $\omega_L$ . For  $\delta \neq 0$ , the detuning of the laser field will be different on each of the  $\pi$  transitions. There are thus two effective Rabi frequencies  $\Omega_1$  and  $\Omega_2$  involved. The splitting of the dressed states for fixed  $N$  is not to scale.

Section III A provides a detailed discussion of the weight of the interference term  $I_{\text{coh}}^{\text{int}}$  in the coherent spectrum. These results can also be applied to the weight of the interference term  $I_{\text{inc}}^{\text{int}}$  in the inelastic spectrum by means of Eq. (34). For example, it follows that the weight of the interference term  $I_{\text{inc}}^{\text{int}}$  in the inelastic spectrum vanishes for  $\delta = \delta_0$ . This situation is shown in Figure 4 b), where the width and the weight of the additional peak is larger than in a). For  $\delta = \delta_{\min}$  and the parameters of Fig. 4, we know from Sec. III A that the weight of the Rayleigh line is approximately zero. The corresponding incoherent spectrum is shown in Fig. c). Instead of the elastic delta-peak in the coherent spectrum we thus have a very narrow peak that occurs in the incoherent spectrum.

Finally, Fig. 4 d) shows  $S_{\text{inc}}^{\pi}$  for a strong laser field. In this case, the weight of the interference terms is negligible as can be verified with the help of Eq. (30). However, the incoherent spectrum still deviates from the Mollow spectrum if  $\delta \neq 0$ . This can be easily understood with the aid of the dressed states [38, 41] of the system. If  $N$  denotes the number of laser photons of frequency  $\omega_L$ , the dressed states can be expressed in terms of the bare states as follows,

$$\begin{aligned} |1(N)\rangle &= e^{i\phi} \sin \Theta_1 |1, N\rangle + \cos \Theta_1 |3, N+1\rangle \\ |2(N)\rangle &= e^{i\phi} \cos \Theta_1 |1, N\rangle - \sin \Theta_1 |3, N+1\rangle \end{aligned} \quad (42)$$

where  $\tan 2\Theta_1 = 2|\Omega|/\Delta$  and

$$\begin{aligned} |3(N)\rangle &= e^{i\phi} \sin \Theta_2 |2, N\rangle - \cos \Theta_2 |4, N+1\rangle \\ |4(N)\rangle &= e^{i\phi} \cos \Theta_2 |2, N\rangle + \sin \Theta_2 |4, N+1\rangle \end{aligned} \quad (43)$$

with  $\tan 2\Theta_2 = 2|\Omega|/(\Delta - \delta)$  ( $0 < \Theta_1, \Theta_2 < \pi/2$ ,  $e^{i\phi} = \Omega/|\Omega|$ ). Figure 5 shows the relative position of the

dressed states for two manifolds with  $N$  and  $(N-1)$  laser photons, respectively. Note that  $|1(N)\rangle$  and  $|2(N)\rangle$  are separated by a frequency interval of  $\Omega_1 = \sqrt{4|\Omega|^2 + \Delta^2}$ , whereas the spacing between  $|3(N)\rangle$  and  $|4(N)\rangle$  is given by  $\Omega_2 = \sqrt{4|\Omega|^2 + (\Delta - \delta)^2}$ . The sidebands in the spectrum of the  $\pi$  transitions result from the transitions  $|1(N)\rangle \rightarrow |2(N-1)\rangle$ ,  $|2(N)\rangle \rightarrow |1(N-1)\rangle$ ,  $|3(N)\rangle \rightarrow |4(N-1)\rangle$  and  $|4(N)\rangle \rightarrow |3(N-1)\rangle$ . Consequently, they will be located at the frequencies  $\omega_L \pm \Omega_1$  and  $\omega_L \pm \Omega_2$ . For  $\delta \neq 0$ , we thus expect four sideband peaks symmetrically placed around the laser frequency  $\omega_L$ , precisely as in Fig. 4 d).

### C. Influence of the interference terms on the fluorescence spectrum

In this Section we investigate how the interference terms alter the fluorescence spectrum emitted on the  $\pi$  transitions. Here we only consider the degenerate system that is distinguished by maximal constructive (destructive) interference in the coherent (incoherent) part of the fluorescence spectrum, see Sec. III. If the interference terms in Eq. (24) are omitted, the fluorescence spectrum reads

$$S_0^{\pi}(\tilde{\omega}) = \frac{1}{\pi} \sum_{i=1}^2 \gamma_{ii} \text{Re} \int_0^{\infty} e^{-i\tilde{\omega}\tau} \langle \tilde{S}_i^+(\tilde{\tau} + \tau) \tilde{S}_i^-(\tilde{\tau}) \rangle_{\text{st}} d\tau. \quad (44)$$

The fluorescence spectra with and without the interference terms according to Eqs. (24) and (44) are shown in Fig. 6 for different parameters of the laser field. If the saturation parameter defined in Eq. (49) is much larger than unity, the weight of the interference terms goes to zero. However, Fig. 6 a) demonstrates that the interference terms still alter the shape of the fluorescence spectrum in the region of the sideband peaks. The spectrum  $S^{\pi}$  with interference terms is identical to the fluorescence spectrum of a two-level atom (see Sec III), and thus the ratio between the central and the sideband peaks reads  $1 : 3 : 1$ . For the spectrum without the interference terms and a branching probability of  $b_{\pi} = 1/3$ , this ratio reads  $7 : 15 : 7$ .

Figure 6 b) shows  $S^{\pi}$  and  $S_0^{\pi}$  for low saturation. In this case, the spectrum without interference terms is distinguished by a narrow peak centered at the laser frequency that occurs in addition to the elastic Rayleigh peak. A numerical analysis shows that  $S_0^{\pi}$  can be written as

$$S_0^{\pi}(\tilde{\omega}) \approx I_{\text{coh}}^0 \delta(\tilde{\omega}) + S_{\text{inc}}^{\pi}(\tilde{\omega}) + S_{\text{peak}}^{\pi}(\tilde{\omega}). \quad (45)$$

In this equation, the first term represents the Rayleigh peak whose weight misses the interference term  $I_{\text{coh}}^{\text{int}}$  that is present in Eq. (35). The second term stands for the incoherent spectrum according to Eq. (40). The last term describes a Lorentzian of weight  $I_{\text{coh}}^{\text{int}}$  and width  $\Gamma_{\pi}$  that

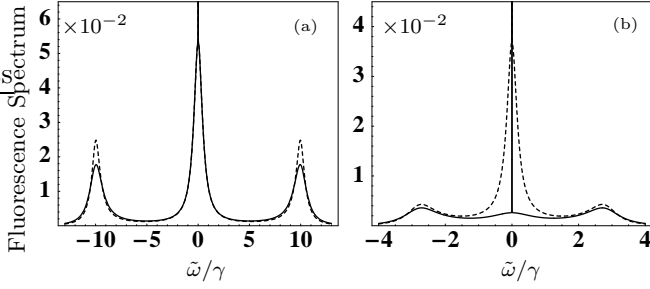


FIG. 6: Fluorescence spectrum for the degenerate system according to Eq. (24). The solid line (dashed line) shows the spectrum with (without) the interference terms proportional to  $\gamma_{12}$ ,  $\gamma_{21}$ . The Rayleigh peak (the vertical line at  $\omega = \omega_L$ ) is present both with and without interference terms. Note that its weight is larger if the interference terms are taken into account. However, the sums of the integrated coherent and incoherent spectra with and without the interference terms are identical, making the total intensity independent of the interference terms. In a), the parameters are  $\Omega = 5 \times 10^7 \text{ s}^{-1}$ ,  $\Delta = 0$  and  $\gamma = 10^7 \text{ s}^{-1}$ . For b), we have  $\Omega = 10^7 \text{ s}^{-1}$ ,  $\Delta = 2 \times 10^7 \text{ s}^{-1}$  and  $\gamma = 10^7 \text{ s}^{-1}$ .

is centered at the laser frequency,

$$S_{\text{peak}}^{\pi}(\tilde{\omega}) = \frac{I_{\text{coh}}^{\text{int}}}{\pi} \frac{\Gamma_{\pi}}{\tilde{\omega}^2 + \Gamma_{\pi}^2}. \quad (46)$$

The weight of the extra peak  $S_{\text{peak}}^{\pi}$  is determined by the constraint that the total intensity is independent of the interference terms (see Sec. III). Therefore,  $S_{\text{peak}}^{\pi}$  has to compensate for the reduced weight of the Rayleigh line of  $S_0^{\pi}$  as compared to the spectrum with interference terms. In general, the width  $\Gamma_{\pi}$  of the extra peak  $S_{\text{peak}}^{\pi}$  is smaller than the decay rate  $\gamma$ . If the saturation parameter  $s$  is much smaller than unity, we find ( $b_{\pi} = 1/3$ )

$$I_{\text{coh}}^{\text{int}} \approx \frac{\gamma}{12}(1-2s)s \quad \text{and} \quad \Gamma_{\pi} \approx 2\frac{\gamma}{9}(3-5s)s. \quad (47)$$

Figure 6 b) allows to summarize the effect of the interference terms on the fluorescence spectrum in the case of low saturation as follows. The spectrum without interference terms displays a narrow peak  $S_{\text{peak}}^{\pi}$  of finite width at the laser frequency that is absent if the interference terms are taken into account. Therefore, quantum interference cancels the incoherent response of the atom at the laser frequency  $\omega_L$ .

In conclusion, the experimental observation of the fluorescence spectrum confirming the solid lines in Fig. 6 would give evidence for vacuum-mediated interference effects as described by terms proportional to  $\gamma_{12}$ . So far, interference effects of this kind have not been observed in atomic systems.

#### IV. SPECTRUM OF RESONANCE FLUORESCENCE II - $\sigma$ TRANSITIONS

This Section is concerned with a brief discussion of the fluorescence spectrum emitted on the  $\sigma$  transitions. Since the laser field does not couple to these transitions, the spectrum contains only an incoherent part. We arrive at

$$S^{\sigma}(\tilde{\omega}) = \phi_{\sigma} \frac{b_{\sigma}\gamma}{\pi} \sum_{i=3}^4 \text{Re} \int_0^{\infty} e^{-i\tilde{\omega}\tau} \langle \delta\tilde{S}_i^+(\hat{t}+\tau) \delta\tilde{S}_i^-(\hat{t}) \rangle_{\text{st}} d\tau, \quad (48)$$

where  $\phi_{\sigma}$  is a geometrical factor that we set equal to one in the following. It has been pointed out in Sec. II that the light emitted on the  $\sigma$  transitions is linearly polarized along  $\mathbf{e}_x$  if the point of observation lies in the  $y$ -direction. Therefore, the cross terms  $\langle \delta\tilde{S}_3^+(\hat{t}+\tau) \delta\tilde{S}_4^-(\hat{t}) \rangle_{\text{st}}$  and  $\langle \delta\tilde{S}_4^+(\hat{t}+\tau) \delta\tilde{S}_3^-(\hat{t}) \rangle_{\text{st}}$  will, in principle, contribute to the spectrum in Eq. (48). However, we find that the latter two-time averages are equal to zero. For different driving schemes where the laser field couples to the  $\sigma$  transitions, the cross-correlation terms have to be taken into account as is the case in the work of Polder et. al. [33]. The exact analytical expression for  $S^{\sigma}$  is too bulky to display it here. Instead we will discuss  $S^{\sigma}$  in the case of the degenerate system ( $B = \delta = 0$ ) and for different regimes of the driving field strength that will be characterized by means of the saturation parameter

$$s = \frac{2|\Omega|^2}{\Delta^2 + \gamma^2/4}. \quad (49)$$

In the range from a weak to a moderately strong laser field ( $s < 1$ ), a numerical analysis reveals that  $S^{\sigma}$  can be written as

$$S^{\sigma}(\tilde{\omega}) \approx b_{\sigma}/b_{\pi} S_{\text{inc}}^{\pi}(\tilde{\omega}) + S_{\text{peak}}^{\sigma}(\tilde{\omega}). \quad (50)$$

In this equation, the first term stands for the incoherent spectrum of a two-level atom according to Eq. (40). The prefactor  $b_{\sigma}/b_{\pi}$  accounts for the different branching probability of the  $\sigma$  transitions as compared to the  $\pi$  transitions. The second term represents a narrow peak that is centered at the laser frequency  $\omega = \omega_L$ . It can be modeled as a Lorentzian of weight  $\mathcal{W}_{\sigma}$  and width  $\Gamma_{\sigma}$ ,

$$S_{\text{peak}}^{\sigma}(\tilde{\omega}) = \frac{\mathcal{W}_{\sigma}}{\pi} \frac{\Gamma_{\sigma}}{\tilde{\omega}^2 + \Gamma_{\sigma}^2}. \quad (51)$$

The weight of  $S_{\text{peak}}^{\sigma}$  is determined by the total intensity emitted on the  $\sigma$  transitions

$$I_{\text{st}}^{\sigma} = b_{\sigma}\gamma(\tilde{\varrho}_{11} + \tilde{\varrho}_{22}) \quad (52)$$

and the weight of  $b_{\sigma}/b_{\pi} S_{\text{inc}}^{\pi}$ . We arrive at

$$\mathcal{W}_{\sigma} = 4b_{\sigma}\gamma|\tilde{\varrho}_{13}|^2, \quad (53)$$

where  $\tilde{\varrho}_{13}$  is given in Eq. (16). The width  $\Gamma_{\sigma}$  of the additional peak is smaller than the decay rate  $\gamma$ . If  $s$

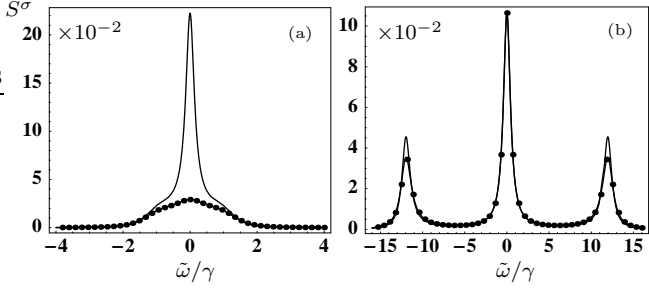


FIG. 7: Spectrum of resonance fluorescence emitted on the  $\sigma$  transitions (solid line) in comparison with the fluorescence spectrum of a two-level atom (dotted line). The parameters in (a) are  $\Omega = 5 \times 10^6 \text{ s}^{-1}$ ,  $\Delta = 6 \times 10^6 \text{ s}^{-1}$  and  $\gamma = 10^7 \text{ s}^{-1}$ . In (b), the parameters are  $\Omega = 6 \times 10^7 \text{ s}^{-1}$ ,  $\Delta = 0$  and  $\gamma = 10^7 \text{ s}^{-1}$ . Note that  $S^\sigma$  deviates slightly from the Mollow triplet in the region of the sideband peaks.

is much smaller than unity, the width and the weight of  $S_{\text{peak}}^\sigma$  are given by

$$\begin{aligned} \mathcal{W}_\sigma &\approx b_\sigma \frac{\gamma}{2} (1 - 2s)s \\ \Gamma_\sigma &\approx b_\sigma \frac{\gamma}{4} [2 - (2 + b_\sigma)s]s. \end{aligned} \quad (54)$$

At the same time, the contribution of  $S_{\text{inc}}^\pi b_\sigma/b_\pi$  to  $S^\sigma$  is small such that the spectrum is dominated by the central narrow peak  $S_{\text{peak}}^\sigma$ . If the field strength is increased, the weight of the extra peak  $S_{\text{peak}}^\sigma$  gets smaller. Figure 7 a) shows  $S^\sigma$  (solid line) and  $S_{\text{inc}}^\pi b_\sigma/b_\pi$  (dotted line) for a moderately strong laser field, the saturation parameter is on the order of unity. Nevertheless, the spectrum  $S^\sigma$  is still dominated by the sharp peak  $S_{\text{peak}}^\sigma$  that exceeds the central peak of the two-level spectrum by one order of magnitude.

For a strong driving field ( $s \gg 1$ ), the weight of  $S_{\text{peak}}^\sigma$  goes to zero and the central peak of  $S^\sigma$  coincides with the corresponding peak of the Mollow spectrum. However, the sideband peaks of  $S^\sigma$  differ from those of a two-level atom as can be seen from Fig. 7 b). In the secular limit, it is advantageous to employ the dressed state picture in order to obtain analytic expressions for the sideband peaks, being well separated from the central peak whose analytic form can be taken over from the well-known results for a two-level atom [38, 40]. The fluorescence spectrum for a resonant driving field can be achieved by a tedious but straightforward calculation that follows the procedure of Chapter VI.E in [38],

$$\begin{aligned} S^\sigma(\tilde{\omega}) &\approx \gamma \frac{b_\sigma}{8\pi} \frac{\Gamma_{\text{sb}}}{\Gamma_{\text{sb}}^2 + (\Omega_1 - \tilde{\omega})^2} \\ &+ \gamma \frac{b_\sigma}{4\pi} \frac{\gamma/2}{\gamma^2/4 + \tilde{\omega}^2} + \gamma \frac{b_\sigma}{8\pi} \frac{\Gamma_{\text{sb}}}{\Gamma_{\text{sb}}^2 + (\Omega_1 + \tilde{\omega})^2}, \end{aligned} \quad (55)$$

where  $\Omega_1 = \sqrt{4|\Omega|^2 + \Delta^2}$ . A comparison of the latter equation with the corresponding expression for the Mollow spectrum reveals that the weights of the sideband

peaks differ only by the branching probability  $b_\sigma$ . For the width of the sideband peaks in Eq. (55) we find

$$\Gamma_{\text{sb}} = \frac{1}{4} \sqrt{\gamma_1 \gamma_2} + \frac{\gamma}{2} = \frac{1}{4} (3 - b_\sigma) \gamma. \quad (56)$$

Note that the second equality is obtained by virtue of Eq. (11). The ratio between the heights of the central peak at  $\tilde{\omega} = 0$  and the sideband peaks at  $\tilde{\omega} = \pm\Omega_1$  is found to be  $3 - b_\sigma$ . For  $b_\sigma = 2/3$ , the peak ratio is thus  $3 : 7 : 3$ . By contrast, the peak ratio of the Mollow spectrum reads  $1 : 3 : 1$ . A precise measurement of the peak ratio would thus provide a means of determining the branching probability  $b_\sigma$  of the degenerate system experimentally.

Note that the width of the sideband peaks in Eq. (56) depends on the cross-damping terms  $\sqrt{\gamma_1 \gamma_2}$  that appear in the master equation through the spontaneous emission term  $\mathcal{L}_\gamma \tilde{\varrho}$  in Eq. (8). If these interference terms were not present, the peak ratio would not depend on the branching probabilities and would be given by  $1 : 2 : 1$ . The spectrum emitted on the  $\sigma$  transitions shows thus an indirect signature of interference.

## V. DISCUSSION

In Section III we have shown that the interference terms proportional to  $\gamma_{12}$  contribute only to the spectrum of resonance fluorescence, but not to the total intensity in Eq. (21). Here we demonstrate that this result is a consequence of the principle of complementarity, applied to time and energy.

If the total intensity is measured, complementarity does not impose any restrictions on the time resolution of the measurement since the photon energies are not observed. It is thus possible to observe the temporal aspect of the radiative cascade, i.e. one could determine the photon emission times. The time evolution of the driven atom is then most suitably described in the bare state basis. For example, assume that the atom is initially in ground state  $|3\rangle$ . The laser field will induce Rabi oscillations between the excited state  $|1\rangle$  and  $|3\rangle$ . Immediately after the spontaneous emission of a photon, the atom is found in ground state  $|3\rangle$  ( $\pi$  transition) or  $|4\rangle$  ( $\sigma$  transition). Subsequently, this sequence of Rabi oscillations and a spontaneous emission event is repeated. In this description, each emission process on one of the  $\pi$  transitions is independent of the other  $\pi$  transition. However, quantum interference does only occur if various indistinguishable transition amplitudes connect a common initial state to a common final state. Since the  $\pi$  transitions do neither share a common initial nor a common final state, we must conjecture that the total intensity is not affected by interference.

The lack of interference in the total intensity can also be explained by drawing an analogy to the two-slit experiment. It is well known that the interference pattern vanishes as soon as it is principally possible to know

through which of the two slits each object (electrons or photons) has moved. Similarly, the internal states of our atom can be regarded as a which-way marker. Since the experimental conditions allow, at least in principle, to determine the atomic ground state immediately after the detection of a  $\pi$ -photon, one could decide on which of the two  $\pi$ -transitions the photon was emitted. Consequently, the observer could reveal the quantum path taken by the system and hence there is no signature of interference. Note that this argument requires that the retardation between the times of emission and detection is much smaller than the time between successive emissions. This condition can typically be achieved in atomic systems.

A totally different situation arises if the detector measures the spectrum of resonance fluorescence and hence the energy of the emitted photons. First of all, it is advantageous to illustrate the energy aspect of the cascade of spontaneously emitted photons in the dressed state picture (see Fig. 8) rather than in the bare state picture. The crucial difference between the measurement of the total intensity and the fluorescence spectrum is the following. In the latter case, the observer decides to determine the photon energies precisely. Since time and energy are complementary observables, the temporal aspect of the radiative cascade is not accessible simultaneously. Next we demonstrate that precisely this lack of information about the temporal sequence of photon emissions allows for the interference mechanism in the fluorescence spectrum.

A quantitative description of time-energy complementarity is achieved via the time-energy uncertainty. If the photon energies are determined with a precision of  $\Delta\omega$ , the time-energy uncertainty relation enforces that the time of observation has to be at least on the order of  $1/\Delta\omega$ . Since the observer can only notice the detection of a photon after the observation time has elapsed, the photon emission times are indeterminate within a time interval of  $\Delta t = 1/\Delta\omega$ . For the moment we envisage an ideal measurement of the fluorescence spectrum. In this case, the atom will emit (infinitely) many photons during the (infinite) time of observation. In addition, the photon emission times are indeterminate, and thus the time order in which these photons have been emitted is unknown. It follows that the transition amplitudes corresponding to the various time orderings of the photons will interfere.

We illustrate this interference mechanism on the basis of Fig. 8 that shows a cascade of only two photons, one emitted on a  $\pi$  transition and the other on a  $\sigma$  transition. Assume that the atom is initially in the dressed state  $|4(N)\rangle$ . In one of the two cascades, the atom decays first to the state  $|4(N-1)\rangle$  by the emission of a  $\pi$  photon on the bare state transition  $|2\rangle \rightarrow |4\rangle$ . The subsequent emission of a  $\sigma$  photon takes the atom to the state  $|1(N-2)\rangle$  within the manifold with  $N-2$  laser photons. In the second cascade, the time order of the two photons is reversed. The atom decays now first to the state  $|1(N-1)\rangle$  by the emission of a  $\sigma$  photon, and

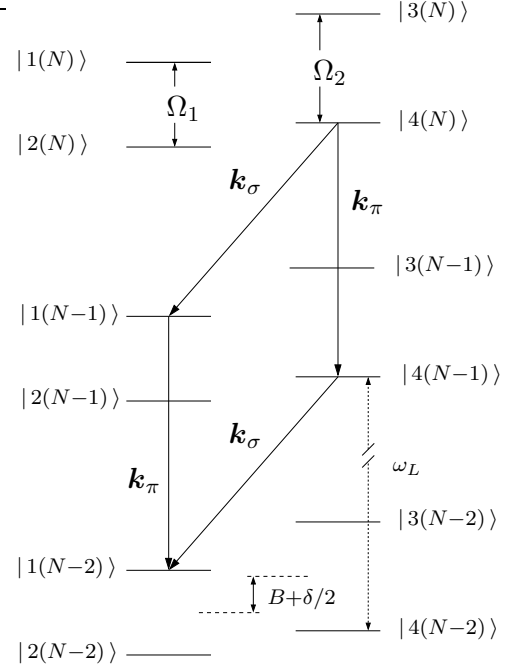


FIG. 8: Radiative cascade in the dressed states of the system [see Eqs. (42) and (43)]. The splitting of the dressed states for a fixed number of laser photons  $N$  is not to scale. Each of the two indicated cascades involves the emission of a  $\pi$  photon and a  $\sigma$  photon with wave vector  $\mathbf{k}_\pi$  and  $\mathbf{k}_\sigma$ , respectively. Depending on the time order of their emission, the  $\pi$  photon is either emitted on transition  $|4(N)\rangle \rightarrow |4(N-1)\rangle$  or  $|1(N-1)\rangle \rightarrow |1(N-2)\rangle$ , corresponding to the bare state transitions  $|2\rangle \rightarrow |4\rangle$  and  $|1\rangle \rightarrow |3\rangle$ , respectively. Since the final and initial states of the two cascades are identical, the corresponding transition amplitudes may interfere.

then to the final state  $|1(N-2)\rangle$  under the emission of a  $\pi$  photon. In contrast to the first cascade, this  $\pi$  photon is now emitted on the bare state transition  $|1\rangle \rightarrow |3\rangle$ . Since the two cascades in Fig. 8 have the same initial and final states, and since it is in principle impossible to determine the quantum path taken by the system, the two transition amplitudes corresponding to different time orders of photon emissions interfere. In one of the transition amplitudes the  $\pi$  photon stems from the  $|2\rangle \rightarrow |4\rangle$  transition, and in the other from the  $|1\rangle \rightarrow |3\rangle$  transition. Exactly this mechanism gives rise to the interference effects in the fluorescence spectrum that are mediated by the cross-damping terms in Eq. (24).

The provided explanation can also be employed to illustrate why there is no interference in the fictitious situation of perpendicular dipole moments  $\mathbf{d}_1$  and  $\mathbf{d}_2$ . In this case, a photon can either stem from  $\mathbf{d}_1$  or  $\mathbf{d}_2$ , but not from both transitions. It is then impossible to realize both cascades in Fig. 8, and hence there is no interference. Moreover, it becomes now clear why the spectrum emitted on the  $\sigma$  transitions depends on the interference terms  $\gamma_{12}$  and  $\gamma_{21}$ . For anti-parallel dipole moments  $\mathbf{d}_1$  and  $\mathbf{d}_2$  there are two transition amplitudes that involve

the emission of a  $\sigma$  photon, and for perpendicular dipole moments there would be only one. We emphasize that the discussion has been restricted to a cascade of only two photons for the sake of simplicity. In principle, all possible cascades with an arbitrary number of photons have to be considered, but the general idea remains the same.

It is also possible to provide an explanation for the interference in the coherent spectrum, but the elastic scattering events cannot be visualized in the dressed state basis. However, in the case of low saturation ( $s \ll 1$ ) the process of elastic scattering can be illustrated in the bare state basis such that the atom hops from one ground state to another by the absorption of a laser photon and the emission of a scattered photon. The excited states act as intermediate states and can be adiabatically eliminated. Since it is impossible to tell on which of the two  $\pi$  transitions the photon was scattered, it is plausible that one has to sum the scattering amplitudes first and then take the absolute value squared in order to obtain the weight of the Rayleigh line in Eq. (38).

Next we demonstrate how the interfering transition amplitudes that correspond to different time orders of photon emissions enter the expression for the spectrum of resonance fluorescence in Eq. (24). Let  $a_\pi$  ( $a_\pi^\dagger$ ) be the annihilation (creation) operator of a photon in a mode of the radiation field that is actually observed by the detector, being sensitive only to photons emitted on the  $\pi$  transitions. The rate at which the photon number in this particular mode changes is given by

$$R_\pi(t) = \partial_t \langle a_\pi^\dagger(t) a_\pi(t) \rangle. \quad (57)$$

If one follows the lines of Chapter 7 in [2], one can show that the steady-state value of  $R_\pi$  is proportional to the spectrum of resonance fluorescence,

$$\lim_{t \rightarrow \infty} R_\pi(t) \sim S^\pi(c |\mathbf{k}_\pi| - \omega_L). \quad (58)$$

In this equation,  $\mathbf{k}_\pi$  denotes the wave vector that corresponds to the observed mode  $a_\pi$ , and  $c$  is the speed of light. In order to evaluate the left hand side of Eq. (58), we will label the basis states  $|i(N); \{n\}\rangle$  of the total system (atom + laser field + vacuum modes) by three quantum numbers, namely the dressed states  $i$ , the number of laser photons  $N$  and the state of the vacuum modes  $\{n\}$ . The mean value on the right hand side of Eq. (57) becomes then

$$\langle a_\pi^\dagger(t) a_\pi(t) \rangle = \sum_{i=1}^4 \sum_{N, \{n\}} |C_{N, \{n\}}^i(t)|^2 N_\pi(\{n\}), \quad (59)$$

where  $|C_{N, \{n\}}^i(t)|^2$  is the probability to find the system at time  $t$  in state  $|i(N); \{n\}\rangle$  and  $N_\pi(\{n\})$  is the expectation value of  $a_\pi^\dagger a_\pi$  in this state. We assume that the system is in some initial state  $|\psi_0\rangle$  at time  $t = 0$  with all vacuum modes being empty. If the time evolution operator is labeled by  $U(t, 0)$ , the transition amplitude from

the initial state  $|\psi_0\rangle$  to the final state  $|i(N); \{n\}\rangle$  can be written as

$$C_{N, \{n\}}^i(t) = \langle i(N); \{n\} | U(t, 0) | \psi_0 \rangle. \quad (60)$$

Let us assume that the final state contains  $q$  scattered photons that are characterized by their wave and polarization vectors,  $\{n\} = \{\mathbf{k}_\pi \epsilon_\pi, \mathbf{k}_2 \epsilon_2, \dots, \mathbf{k}_q \epsilon_q\}$ . We do not attempt to evaluate Eq. (60) explicitly, but in principle one would introduce  $q - 1$  intermediate states and arrange the  $q$  scattered photons into a certain order. But since there is no distinguished time order of the scattered photons, there are, in principle,  $q!$  transition amplitudes involved in the evaluation of Eq. (60) that will all interfere.

In conclusion, we demonstrated that the interference in the spectrum from the  $\pi$  transitions can be explained in terms of interference between transition amplitudes that correspond to different time orders of photon emissions. If the spectrum of resonance fluorescence is observed, the principle of complementarity enforces that these transition amplitudes are indistinguishable. If the total intensity is recorded by a broadband detector, the temporal aspect of the radiative cascade can in principle be observed. Consequently, the possibility of interference between different time orders of photon emissions is ruled out. The preceding discussion of our results also implies that the experimental setup—potentially after the photon emissions—decides if interference takes place, a feature that is also known from quantum eraser schemes [42, 43].

We now refine our analysis and consider a detector with a finite frequency resolution  $\Delta\omega$  that allows us to study the continuous transition from perfect frequency resolution to perfect time resolution. For simplicity, we consider only the degenerate system ( $B = \delta = 0$ ). If a filter of bandwidth  $\lambda$  and setting frequency  $\omega$  is placed in front of a broadband detector, the spectrum can be determined with an accuracy of  $\lambda$ , and the temporal resolution is on the order of  $\lambda^{-1}$ . The spectrum of resonance fluorescence emitted on the  $\pi$  transitions reads then [44]

$$S^\pi(\tilde{\omega}, \lambda) = \frac{1}{\pi} \sum_{i, j=1}^2 \gamma_{ij} \operatorname{Re} \int_0^\infty e^{-i\tilde{\omega}\tau} e^{-\lambda\tau} \langle \tilde{S}_i^+(\hat{t} + \tau) \tilde{S}_j^-(\hat{t}) \rangle_{\text{st}} d\tau. \quad (61)$$

In the absence of interference terms the spectrum will be denoted by  $S_0^\pi(\tilde{\omega}, \lambda)$  and is obtained from Eq. (61) by omitting the terms proportional to  $\gamma_{12}$  and  $\gamma_{21}$ . For the rest of this Section we assume that the saturation parameter  $s$  is much smaller than unity. To a first approximation, the incoherent contribution to the spectrum with interference terms can then be neglected. In the presence of the filter, the coherent  $\delta$ -peak becomes a Lorentzian of width  $\lambda$  and weight  $I_{\text{coh}}^0 + I_{\text{coh}}^{\text{int}}$ , and thus we obtain

$$S^\pi(\tilde{\omega}, \lambda) \approx \frac{I_{\text{coh}}^0 + I_{\text{coh}}^{\text{int}}}{\pi} \frac{\lambda}{\tilde{\omega}^2 + \lambda^2}. \quad (62)$$

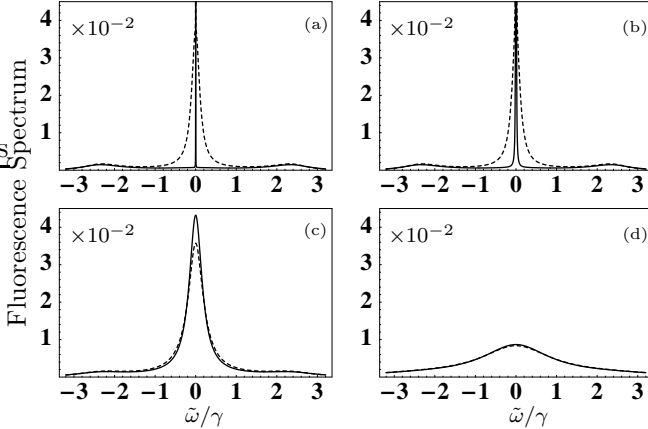


FIG. 9: The solid lines show the fluorescence spectra recorded with a finite frequency resolution  $\lambda$ . The dashed curves are the spectra without the interference terms proportional to  $\gamma_{12}$ ,  $\gamma_{21}$  in Eq. (61). The parameters are  $\Omega = 7 \times 10^6 s^{-1}$ ,  $\Delta = 2 \times 10^7 s^{-1}$ ,  $\gamma = 10^7 s^{-1}$  and  $B = \delta = 0$ . This corresponds to a saturation parameter of  $s = 0.235$  and a mean number of photons per unit time of approximately  $9.4 \times 10^5 s^{-1}$ . The filter bandwidths are given by a)  $\lambda = 10^2 s^{-1}$ , b)  $\lambda = 10^4 s^{-1}$ , c)  $\lambda = 1.9 \times 10^6 s^{-1}$  and d)  $\lambda = 10^7 s^{-1}$ .

Similarly, we neglect the contribution of  $S_{\text{inc}}^{\pi}$  to the spectrum without interference terms in Eq. (45), the  $\delta$ -peak becomes a Lorentzian of width  $\lambda$  and weight  $I_{\text{coh}}^0$ , and  $S_{\text{peak}}^{\pi}$  is replaced by a Lorentzian of width  $\Gamma_{\pi} + \lambda$  and weight  $I_{\text{coh}}^{\text{int}}$ ,

$$S_0^{\pi}(\tilde{\omega}, \lambda) \approx \frac{I_{\text{coh}}^0}{\pi} \frac{\lambda}{\tilde{\omega}^2 + \lambda^2} + \frac{I_{\text{coh}}^{\text{int}}}{\pi} \frac{\Gamma_{\pi} + \lambda}{\tilde{\omega}^2 + (\Gamma_{\pi} + \lambda)^2}. \quad (63)$$

Figure 9 shows the fluorescence spectrum according to Eq. (61) (solid lines) for different values of the filter bandwidth  $\lambda$  and for low saturation. The dashed lines are the spectra without the interference terms. In Fig. 9 a), the bandwidth  $\lambda$  is much smaller than  $\Gamma_{\pi}$ . Therefore, the widths of the lines  $S^{\pi}(\tilde{\omega}, \lambda)$  and  $S_0^{\pi}(\tilde{\omega}, \lambda)$  are clearly distinct. If  $\lambda$  is increased, the differences between the spectra with and without the interference terms diminish until both curves are virtually identical for  $\lambda = \gamma$  (Fig. 9 d)).

These results can be understood as follows. With an increasing filter bandwidth  $\lambda$ , the smallest time interval  $\Delta t$  that can be resolved by the detector without violating the time-energy uncertainty gets shorter. Therefore, the observer can in principle obtain more information about the quantum path taken by the atom. Consequently, we expect that the signature of interference in the fluorescence spectrum diminishes for increasing  $\lambda$ . This is in agreement with Fig. 9 and completely analogous to a two-slit experiment, where the visibility of the interference pattern is reduced at the cost of which-path information and vice versa [45].

Furthermore, we demonstrate that the time-energy uncertainty relation allows to estimate the smallest filter

bandwidth  $\lambda$  for which the spectra with and without interference terms should be indistinguishable. Since the total number of photons emitted per unit time is equal to  $\gamma(\tilde{\varrho}_{11} + \tilde{\varrho}_{22})$ , the mean time between successive photon emissions is determined by  $\bar{\Theta} = 1/[\gamma(\tilde{\varrho}_{11} + \tilde{\varrho}_{22})]$ . If the bandwidth  $\lambda$  is chosen such that the temporal resolution could be much better than the mean time between successive photon emissions, i.e.  $\lambda^{-1} \ll \bar{\Theta} = 1/[\gamma(\tilde{\varrho}_{11} + \tilde{\varrho}_{22})]$ , we have

$$\lambda \gg \gamma(\tilde{\varrho}_{11} + \tilde{\varrho}_{22}) \approx (1 - s)s\gamma/2. \quad (64)$$

Under these conditions, the radiative cascade of photons could be observed in a time resolved way and it is extremely unlikely that more than one spontaneous emission takes place during the time of observation. Since this rules out the interference mechanism as described in Sec. V, the signature of interference in the fluorescence spectrum should disappear. But if inequality (64) holds, it follows that  $\lambda \gg \Gamma_{\pi}$ , and in this case  $S^{\pi}(\tilde{\omega}, \lambda)$  and  $S_0^{\pi}(\tilde{\omega}, \lambda)$  are indeed indistinguishable as can be seen from Eqs. (62) and (63). This is confirmed by Fig. 9 d) that shows  $S_0^{\pi}(\tilde{\omega}, \lambda)$  and  $S^{\pi}(\tilde{\omega}, \lambda)$  for a bandwidth  $\lambda$  that is about ten times larger than the mean number of photons emitted per unit time. The two spectra are now virtually indistinguishable.

It remains to explain the sharp peaks in the incoherent spectrum. To this end we return to Fig. 4 that shows the incoherent spectrum  $S_{\text{inc}}^{\pi}$  for several values of the parameter  $\delta$ . A narrow central peak occurs only in case of the non-degenerate system ( $\delta \neq 0$ ), and thus only if the weight of the Rayleigh line deviates from its maximal value attained at  $\delta = 0$ . Therefore, the narrow central peak in the incoherent spectrum may be regarded as a (partially) broadened coherent peak. This broadening can be understood as follows. Except for  $\delta = 0$ , the two  $\pi$  transitions are not equivalent since the absolute value and the phase of the coherences  $\langle \tilde{S}_1^+ \rangle_{\text{st}}$  and  $\langle \tilde{S}_2^+ \rangle_{\text{st}}$  will be different. The time that the atom spends on the  $1 \leftrightarrow 3$  transition can thus be regarded as a dark period with respect to the  $2 \leftrightarrow 4$  transition and vice versa. This suggests that the sharp peaks in the incoherent spectrum can be explained in terms of electron shelving [46, 47, 48]. This explanation is also applicable to the sharp peak in

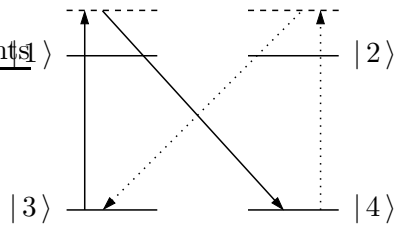


FIG. 10: Schematic representation of elastic scattering events into the  $3 \rightarrow 1 \rightarrow 4$  (solid arrows) and  $4 \rightarrow 2 \rightarrow 3$  channels (dotted arrows). These processes account for the sharp peak in the fluorescence spectrum  $S^{\sigma}$  emitted on the  $\sigma$  transitions.

the spectrum from the  $\sigma$  transitions. Figure 10 illustrates the scattering events that give rise to this peak. If the atom is initially in state  $|3\rangle$ , a scattering event can bring it to state  $|4\rangle$  (solid arrows). The scattered photon has then been emitted on one of the  $\sigma$  transitions. Before the next photon can be scattered on that same transition, a similar scattering process has to take place into the  $4 \rightarrow 2 \rightarrow 3$  channel (dotted arrows). Consequently, every emission on one of the  $\sigma$  transitions is followed by a dark period on that same transition.

It should be mentioned that related interference effects between transition amplitudes corresponding to different time orders of photon emissions do also play a role in the fluorescence spectrum of other systems [49]. However, the distinguished feature of the system presented here is that this mechanism gives rise to interference effects between the two  $\pi$  transitions that do not share a common state.

We also point out that our system belongs to a class of setups that display interference and complementarity in the time-energy domain. In a conventional double-slit experiment, spatially separated pathways result in an interference pattern in position space. This is in contrast to our setup, where different temporal paths lead to interference in the energy domain. The work presented here is thus related to recent double-slit experiments in the time-energy domain [50, 51]. In these experiments, ultra-short laser pulses of atto- or femtosecond duration open different time windows for the photoionization of an atom. If the energy spectrum of the photoelectrons is measured, these time-slits are indistinguishable and an interference pattern is observed. Moreover, it has been demonstrated that interference in the time-energy domain can occur in the intensity correlations of different spectral components in a two-level atom [52, 53, 54].

## VI. SUMMARY

The key result of this paper is that there is quantum interference in the spectrum of resonance fluorescence under conditions of no interference in the total intensity, being enforced by the principle of complementarity. For the system considered here, it claims that it is impossible to observe the temporal and the energy aspect of the radiative cascade of the atom at the same time. If the fluorescence spectrum is observed, the photon emission times are indeterminate. The interference in the fluorescence spectrum can thus be explained in terms of interferences between transition amplitudes that correspond to different time orders of photon emissions.

It has been shown that the degree of interference in the fluorescence spectrum emitted on the  $\pi$  transitions can be controlled by means of an external magnetic field. In particular, the degree of interference in the coherent part of the spectrum can be adjusted from perfect constructive to perfect destructive interference. Under conditions of perfect destructive interference, the weight of the

Rayleigh line is completely suppressed. If the difference  $\delta$  between the resonance frequencies of the  $\pi$  transitions is different from zero, the incoherent spectrum emitted on the  $\pi$  transitions contains a very narrow peak whose width is smaller than the decay rate  $\gamma$ . This peak has been identified as a partially broadened coherent peak and can be explained in terms of electron shelving.

The spectrum emitted on the  $\sigma$  transitions contains only an incoherent part. In the case of a weak driving field and for the degenerate system, the fluorescence spectrum displays a narrow peak that can be regarded as broadened coherent peak. For a strong driving field, the widths of the sideband peaks differ from the Mollow spectrum. We have shown that the ratio between the peak heights of the central and the sideband peaks display an indirect signature of interference. In addition, a measurement of the relative peak heights allows to determine the branching probability  $b_\sigma$  of the spontaneous decay of each excited state into the  $\sigma$  channel.

## Acknowledgments

MK thanks Z. Ficek for helpful discussions.

## APPENDIX: CALCULATION OF THE TWO-TIME AVERAGES

In this section we outline how the functions

$$S_{ij}(\tilde{\omega}) = \text{Re} \int_0^\infty e^{-i\tilde{\omega}\tau} \langle \delta\tilde{S}_i^+(\hat{t}+\tau) \delta\tilde{S}_j^-(\hat{t}) \rangle_{\text{st}} d\tau. \quad (\text{A.1})$$

can be evaluated by means of the quantum regression theorem [55, 56]. To this end we introduce the operators  $\mathcal{A}_{ij}$  that are connected to the atomic transition operators  $A_{ij}$  (taken in the Schrödinger picture) by

$$\mathcal{A}_{ij} = W^\dagger A_{ij} W, \quad (\text{A.2})$$

where the unitary transformation  $W$  is defined in Eq. (5). In particular, the operators  $\tilde{S}_i^\pm$  introduced in Sec. (II) can be identified with the operators  $\mathcal{A}_{ij}$  according to

$$\tilde{S}_1^+ = \mathcal{A}_{13} \quad \tilde{S}_2^+ = \mathcal{A}_{24} \quad \tilde{S}_3^+ = \mathcal{A}_{23} \quad \tilde{S}_4^+ = \mathcal{A}_{14}. \quad (\text{A.3})$$

The corresponding Heisenberg operators are then defined as

$$\mathcal{A}_{ij}(t) = U^\dagger(t, 0) \mathcal{A}_{ij} U(t, 0), \quad (\text{A.4})$$

and the time evolution operator has been labeled by  $U$ . A straightforward calculation shows that the mean values of the these Heisenberg operators are directly related to the matrix elements of the reduced density operator  $\tilde{\varrho}$  in the rotating frame,

$$\langle \mathcal{A}_{ij}(t) \rangle = \text{Tr}_A [A_{ij} \tilde{\varrho}(t)] = \tilde{\varrho}_{ji}(t). \quad (\text{A.5})$$

In this equation,  $\text{Tr}_A[\cdot]$  denotes the trace over atomic degrees of freedom. Next we arrange the operators  $\mathcal{A}_{ij}$  in a column vector

$$\mathbf{L} = (\mathcal{A}_{11}, \mathcal{A}_{21}, \mathcal{A}_{31}, \mathcal{A}_{41}, \mathcal{A}_{12}, \mathcal{A}_{22}, \mathcal{A}_{32}, \mathcal{A}_{42}, \mathcal{A}_{13}, \mathcal{A}_{23}, \mathcal{A}_{33}, \mathcal{A}_{43}, \mathcal{A}_{14}, \mathcal{A}_{24}, \mathcal{A}_{34})^t$$

such that  $\langle \mathbf{L}(t) \rangle$  coincides with the Bloch vector  $\mathbf{R}(t)$  of Eq. (14), i.e.  $\langle \mathbf{L}(t) \rangle = \mathbf{R}(t)$ . It follows that the mean values  $\langle \mathbf{L}(t) \rangle$  obey the generalized Bloch Equation (12). If we decompose each component of  $\mathbf{L}$  in mean values and fluctuations according to  $\mathcal{A}_{ij} = \delta\mathcal{A}_{ij} + \langle \mathcal{A}_{ij} \rangle_{\text{st}} \hat{1}$ , we can cast  $\langle \mathbf{L} \rangle$  into the form

$$\langle \mathbf{L}(t) \rangle = \langle \delta\mathbf{L}(t) \rangle + \langle \mathbf{L} \rangle_{\text{st}}, \quad (\text{A.6})$$

where  $\langle \mathbf{L} \rangle_{\text{st}} = \mathbf{R}_{\text{st}} = -\mathcal{M}^{-1}\mathbf{I}$ . If Eq. (A.6) is plugged into Eq. (12) we obtain a homogeneous equation of motion for the fluctuations,

$$\partial_t \langle \delta\mathbf{L}(t) \rangle = \mathcal{M} \langle \delta\mathbf{L}(t) \rangle. \quad (\text{A.7})$$

The two-time correlation functions  $\langle \delta L_i(\hat{t} + \tau) \delta L_j(\hat{t}) \rangle$  for  $i \in \{1, \dots, 15\}$  and fixed  $j$  can be written in vector notation as  $\mathbf{g}^j(\hat{t}, \tau) = \langle \delta\mathbf{L}(\hat{t} + \tau) \delta L_j(\hat{t}) \rangle$ . According to the quantum regression theorem,  $\mathbf{g}^j$  obeys the same equation of motion than the one-time averages  $\langle \delta\mathbf{L}(t) \rangle$ ,

$$\partial_\tau \mathbf{g}^j = \mathcal{M} \mathbf{g}^j \quad \text{for } \tau \geq 0. \quad (\text{A.8})$$

If  $\mathbf{G}^j(\hat{t}, z)$  denotes the Laplace transform of  $\mathbf{g}^j(\hat{t}, \tau)$  with respect to  $\tau$ , it follows

$$\mathbf{G}^j(\hat{t}, z) = [\hat{1} - \mathcal{M}]^{-1} \mathbf{g}^j(\hat{t}, 0). \quad (\text{A.9})$$

We need the Laplace transform at  $z = i\tilde{\omega}$  in steady state to determine the functions  $S_{ij}(\tilde{\omega})$  of Eq. (A.1). With the definitions

$$\mathbf{R}^j = \lim_{\hat{t} \rightarrow \infty} \mathbf{g}^j(\hat{t}, 0) \quad \text{and} \quad \mathbf{K}^j(\tilde{\omega}) = \lim_{\hat{t} \rightarrow \infty} \mathbf{G}^j(\hat{t}, z = i\tilde{\omega}) \quad (\text{A.10})$$

we arrive at

$$\mathbf{K}^j(\tilde{\omega}) = [i\tilde{\omega} \hat{1} - \mathcal{M}]^{-1} \mathbf{R}^j. \quad (\text{A.11})$$

The relevant correlation functions that are needed for the evaluation of Eq. (36) and (48) are then given by

$$\begin{aligned} S_{11}(\tilde{\omega}) &= \text{Re} [\mathbf{K}^3(\tilde{\omega})]_9 & S_{21}(\tilde{\omega}) &= \text{Re} [\mathbf{K}^3(\tilde{\omega})]_{14} \\ S_{22}(\tilde{\omega}) &= \text{Re} [\mathbf{K}^8(\tilde{\omega})]_{14} & S_{12}(\tilde{\omega}) &= \text{Re} [\mathbf{K}^8(\tilde{\omega})]_9 \\ S_{33}(\tilde{\omega}) &= \text{Re} [\mathbf{K}^7(\tilde{\omega})]_{10} & S_{44}(\tilde{\omega}) &= \text{Re} [\mathbf{K}^4(\tilde{\omega})]_{13}. \end{aligned} \quad (\text{A.12})$$

Finally, we remark that Eq. (61) can be evaluated if one replaces  $i\tilde{\omega}$  in Eq. (A.11) by  $i\tilde{\omega} + \lambda$ .

---

[1] Z. Ficek and S. Swain, *Quantum Interference and Coherence* (Springer, 2005).

[2] G. S. Agarwal, *Quantum Statistical Theories of Spontaneous Emission and their Relation to Other Approaches*, Springer Tracts in Modern Physics Vol. 70 (Springer, 1974).

[3] H. Lee, P. Polynkin, M. O. Scully, and S.-Y. Zhu, Phys. Rev. A **55**, 4454 (1997).

[4] S.-Y. Zhu, R. C. F. Chan, and C. P. Lee, Phys. Rev. A **52**, 710 (1995).

[5] S.-Y. Zhu and M. O. Scully, Phys. Rev. Lett. **76**, 388 (1996).

[6] E. Paspalakis and P. L. Knight, Phys. Rev. Lett. **81**, 293 (1998).

[7] E. Paspalakis, C. H. Keitel, and P. L. Knight, Phys. Rev. A **58**, 4868 (1998).

[8] C. H. Keitel, Phys. Rev. Lett. **83**, 1307 (1999).

[9] F. Plastina and F. Piperno, Phys. Rev. A **62**, 053801 (2000).

[10] D. A. Cardimona, M. G. Raymer, and J. C. R. Stroud, J. Phys. B **15**, 55 (1982).

[11] G. C. Hegerfeldt and M. B. Plenio, Phys. Rev. A **46**, 373 (1992).

[12] P. Zhou and S. Swain, Phys. Rev. Lett. **77**, 3995 (1996).

[13] P. Zhou and S. Swain, Phys. Rev. A **56**, 3011 (97).

[14] S. Swain, P. Zhou, and Z. Ficek, Phys. Rev. A **61**, 043410 (2000).

[15] S.-Y. Gao, F.-L. Li, and S.-Y. Zhu, Phys. Rev. A **66**, 43806 (2002).

[16] H.-R. Xia, C.-Y. Ye, and S.-Y. Zhu, Phys. Rev. Lett. **77**, 1032 (1996).

[17] L. Li, X. Wang, J. Yang, G. Lazarov, J. Qi, and A. M. Lyyra, Phys. Rev. Lett. **84**, 4016 (2000).

[18] M. V. G. Dutt, J. Cheng, B. Li, X. Xu, X. Li, P. R. Berman, D. G. Steel, A. S. Bracker, D. Gammon, S. E. Economou, et al., Phys. Rev. Lett. **94**, 227403 (2005).

[19] R. P. Feynman, R. B. Leighton, and M. Sands, *The Feynman Lectures on Physics*, vol. III (Addison-Wesley, 1963).

[20] N. Bohr, in *Albert Einstein: Philosopher-Scientist*, edited by P. A. Schilpp (Library of Living Philosophers, Evanston, 1949), pp. 200-241; reprinted in *Quantum Theory and Measurement*, edited by J. A. Wheeler and W. H. Zurek (Princeton University Press, Princeton, 1983), pp. 8-49.

[21] M. O. Scully, B.-G. Englert, and H. Walther, Nature **351**, 111 (1991).

[22] P. Storey, S. Tan, M. Collett, and D. Walls, Nature **367**, 626 (1994).

[23] B.-G. Englert, M. O. Scully, and H. Walther, Nature **375**, 367 (1995).

[24] E. P. Storey, S. M. Tan, M. J. Collett, and D. F. Walls, Nature **375**, 368 (1995).

[25] H. Wiseman and F. Harrison, Nature **377**, 584 (1995).

[26] H. M. Wiseman, F. E. Harrison, M. J. Collett, S. M. Tan, D. F. Walls, and R. B. Killip, Phys. Rev. A **56**, 55 (1997).

- [27] S. Dürr, T. Nonn, and G. Rempe, *Nature* **395**, 33 (1998).
- [28] A. Luis and L. L. Sánchez-Soto, *J. Opt. B: Quantum Semiclass. Opt.* **1**, 668 (1999).
- [29] U. Eichmann, J. C. Bergquist, J. J. Bollinger, J. M. Gilligan, W. M. Itano, D. J. Wineland, and M. G. Raizen, *Phys. Rev. Lett.* **70**, 2359 (1993).
- [30] T. Wong, S. M. Tan, M. J. Collett, and D. F. Walls, *Phys. Rev. A* **55**, 1288 (1997).
- [31] W. M. Itano, J. C. Bergquist, J. J. Bollinger, D. J. Wineland, U. Eichmann, and M. G. Raizen, *Phys. Rev. A* **57**, 4176 (1998).
- [32] G. S. Agarwal, J. von Zanthier, C. Skornia, and H. Walther, *Phys. Rev. A* **65**, 053826 (2002).
- [33] D. Polder and M. F. H. Schuurmans, *Phys. Rev. A* **14**, 1468 (1976).
- [34] M. Jakob and J. Bergou, *Phys. Rev. A* **60**, 4179 (1999).
- [35] N. Lütkenhaus, J. I. Cirac, and P. Zoller, *Phys. Rev. A* **57**, 548 (1998).
- [36] M. Kiffner, J. Evers, and C. H. Keitel, *Phys. Rev. Lett.* in print.
- [37] J. J. Sakurai, *Modern Quantum Mechanics* (Addison-Wesley, 1994).
- [38] C. Cohen-Tannoudji, J. Dupont-Roc, and G. Grynberg, *Atom-Photon Interactions* (J. Wiley & Sons, 1998).
- [39] B. R. Mollow, *J. Phys. A* **8**, L130 (1975).
- [40] H. J. Kimble and L. Mandel, *Phys. Rev. A* **13**, 2123 (1976).
- [41] C. Cohen-Tannoudji and S. Reynaud, *J. Phys. B* **10**, 345 (1977).
- [42] Y.-H. Kim, R. Yu, S. P. Kulik, Y. Shih, and M. O. Scully, *Phys. Rev. Lett.* **84**, 1 (2000).
- [43] S. P. Walborn, M. O. Terra Cunha, S. Pádua, and C. H. Monken, *Phys. Rev. A* **65**, 033818 (2002).
- [44] J. H. Eberly and K. Wódkiewicz, *J. Opt. Soc. Am.* **67**, 1252 (1977).
- [45] B.-G. Englert, *Phys. Rev. Lett.* **77**, 2154 (1996).
- [46] G. C. Hegerfeldt and M. B. Plenio, *Phys. Rev. A* **52**, 3333 (1995).
- [47] M. B. Plenio and P. L. Knight, *Rev. Mod. Phys.* **70**, 101 (1998).
- [48] J. Evers and C. H. Keitel, *Phys. Rev. A* **65**, 33813 (2002).
- [49] In the case of the radiative cascade of a harmonic oscillator, see, for example, exercise 15 in [38]. For a discussion of related interference effects in the fluorescence spectrum of a two-level atom, see M. E. Smithers and H. S. Freedhoff, *J. Phys. B* **8**, 2911 (1975); Section 2.2.3. in C. Cohen-Tannoudji, *Atoms in strong resonant fields*, in: *Frontiers in Laser Spectroscopy*, Les Houches Session XXVII (1975) (North-Holland, 1977).
- [50] F. Lindner, M. G. Schätzel, H. Walther, A. Baltuška, E. Goulielmakis, F. Krausz, D. B. Milošević, D. Bauer, W. Becker, and G. G. Paulus, *Phys. Rev. Lett.* **95**, 040401 (2005).
- [51] M. Wollenhaupt, A. Prakelt, C. Sarpe-Tudoran, D. Liese, and T. Baumert, *J. Opt. B: Quantum Semiclass. Opt.* **7**, 270 (2005).
- [52] A. Aspect, G. Roger, S. Reynaud, J. Dalibard, and C. Cohen-Tannoudji, *Phys. Rev. Lett.* **45**, 617 (1980).
- [53] C. A. Schrama, G. Nienhuis, H. A. Dijkerman, C. Steijger, and H. G. M. Heideman, *Phys. Rev. Lett.* **67**, 2443 (1991).
- [54] C. A. Schrama, G. Nienhuis, H. A. Dijkerman, C. Steijger, and H. G. M. Heideman, *Phys. Rev. A* **45**, 8045 (1992).
- [55] M. Lax, *Phys. Rev.* **129**, 2342 (1963).
- [56] H. Carmichael, *An Open Systems Approach to Quantum Optics* (Springer, 1993).